

Recording Rotational and Translational Ground Motions of Two TAIGER Explosions in Northeastern Taiwan on 4 March 2008

by Chin-Jen Lin, Chun-Chi Liu, and William H. K. Lee

Abstract Two explosions were set off on 4 March 2008 at the N3 explosion site in northeastern Taiwan. The code name for the first shot with 3000 kg explosives is N3P and that for the second shot with 750 kg explosives is N3. To record these two explosions, 8 triaxial rotational sensors, 13 triaxial accelerometers, and 12 six-channel, 24 bit dataloggers with Global Positioning System receivers were deployed to continuously record several hours before and after the explosions. These instruments were installed at about 250 m (1 station), 500 m (11 stations), and 600 m (1 station) from the explosions. The 11 stations form a center array with station spacing of about 5 m.

Except for one rotational sensor, onscale records were obtained. Although the N3P shot used four times larger amounts of explosives than those used for the N3 shot, the peak ground translational acceleration and rotational velocity at the 13 station sites from the N3P shot are only about 1.5 times larger than those for the N3 shot. We also observed large variations (by tens of percent) of translational accelerations and rotational velocities at the center array with station spacing of about 5 m. The largest peak rotational velocity was observed for the x component: 2.74 and 1.75 mrad/sec at a distance of 254 m from the N3P and N3 shots, respectively.

The main purpose of this article is to document our recordings of rotational and translation motions from two explosions in Taiwan and to release the data online for open access. The translational acceleration data from this experiment have been analyzed by Langston *et al.* (2009), and we plan to submit an article with analysis of the rotational velocity data in the future.

Introduction

The TAIGER (TAiwan Integrated GEodynamics Research) project for testing models of Taiwan orogeny is a collaborative project of 13 institutes (six from the United States, one from Canada, and six from Taiwan) under the leadership of Francis T. Wu (TAIGER, 2008). The ongoing TAIGER project calls for a comprehensive set of geophysical experiments to determine the locations and moment tensors of earthquakes and to obtain multiscale images of the crust and upper mantle. The TAIGER experiments include two seismic refraction/reflection surveys using explosives on land, which were executed in February and March of 2008. We deployed an array of 13 accelerometers and 8 rotational sensors near the N3 explosion site in the Lan-Yang river valley in order to observe both translational and rotational ground motions in the vicinity (~500 m) of the two N3 explosions.

From classical mechanics, three-component translational (T_x , T_y , and T_z) and three-component rotational motions (θ_x , θ_y , and θ_z) are required to describe the motion of a rigid body (Evans and International Working Group on Rotational Seismology, 2009), and six-component strains are

also required for a deformed body (Bath, 1979). According to Cochard *et al.* (2006), displacement \mathbf{u} of a point \mathbf{x} is related to a neighboring point $\mathbf{x} + \delta\mathbf{x}$ by

$$\mathbf{u}(\mathbf{x} + \delta\mathbf{x}) = \mathbf{u}(\mathbf{x}) + \boldsymbol{\epsilon}\delta\mathbf{x} + \boldsymbol{\omega} \times \delta\mathbf{x}, \quad (1)$$

where $\boldsymbol{\epsilon}$ is the strain tensor and

$$\boldsymbol{\omega} = \frac{1}{2} \nabla \times \mathbf{u}(\mathbf{x}) \quad (2)$$

is a pseudovector and represents the angle of rigid rotation generated by the disturbance. At the Earth's surface, it can be shown that the three components of rotation about the x axis, y axis, and z axis are given by the following equations, respectively:

$$\begin{aligned} \omega_x &= \partial u_z / \partial y, & \omega_y &= -\partial u_z / \partial x, \\ \omega_z &= \frac{1}{2} (\partial u_x / \partial y - \partial u_y / \partial x). \end{aligned} \quad (3)$$

Therefore, rotational ground motions can be measured by (1) an array of translational accelerometers indirectly (e.g., Spudich *et al.*, 1995; Huang, 2003; Spudich and Fletcher, 2008), or (2) rotational sensors directly (e.g., Nigbor, 1994; Takeo, 1998; Huang *et al.*, 2006).

Our field recording experiment was motivated by the desire to observe both rotational and translational ground motions. Because we do not know when an earthquake will occur, scheduled explosions offer a quick return of data from a temporary deployment of instruments in the field. By deploying an array of rotational sensors and translational accelerometers, we can observe rotational ground motions directly

and indirectly. Because seismic waves from explosions have more high-frequency contents than typical earthquakes, the translational accelerometer array for recording explosions must have small station spacing (~ 10 m), and thus also allows us to study the variations of ground acceleration in meter scale, rather than the traditional kilometer scale. The prominent frequency from the observed acceleration records was found after the experiment to be about 43 Hz for the vertical component.

The main purpose of this article is to document our recordings of rotational and translation motions from two explosions in Taiwan. All relevant data we collected will be

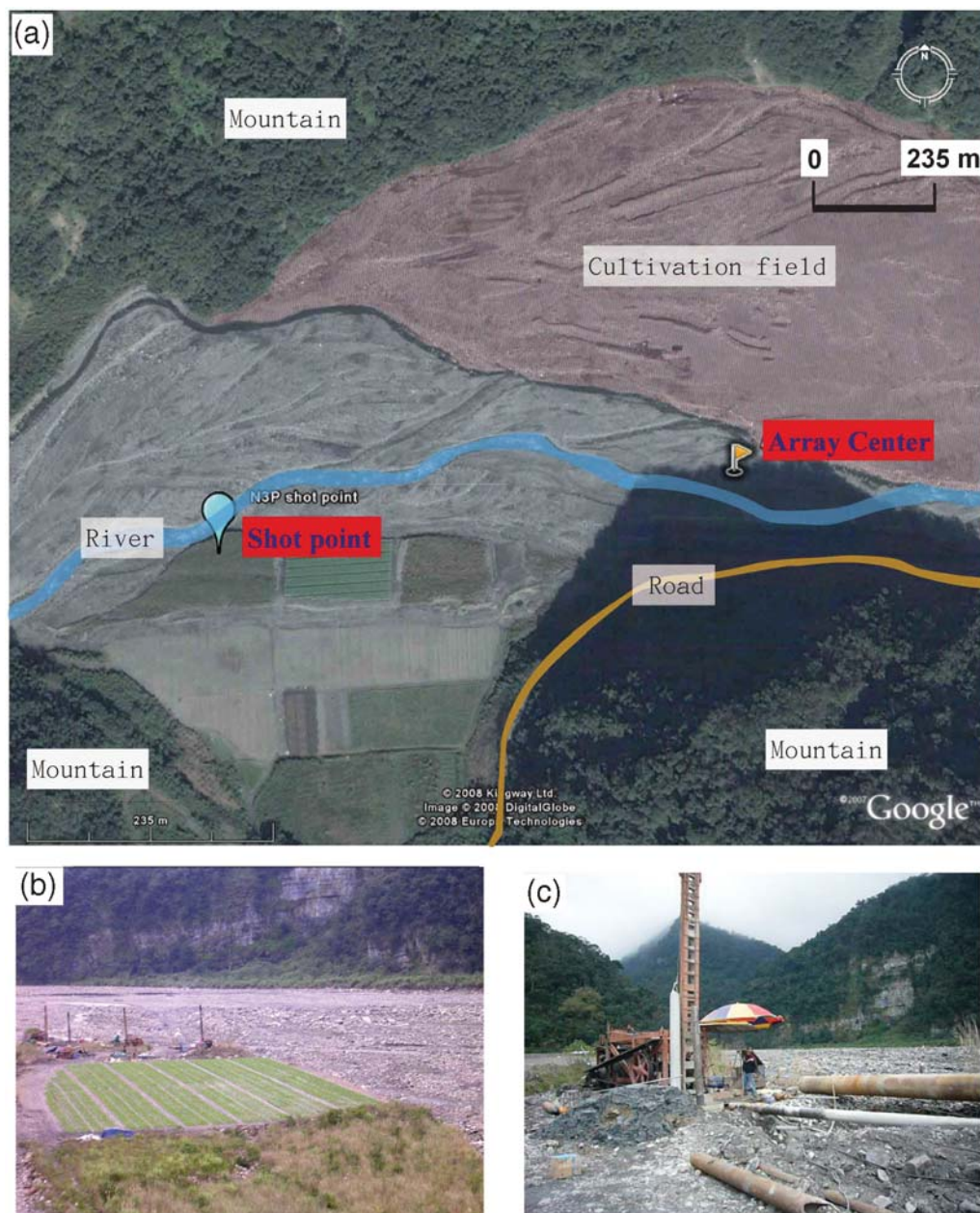


Figure 1. (a) Google map with the N3 explosion site and the array recording site marked and local features noted. (b) A photo of the four boreholes at the N3 explosion site as viewed from the road depicted on (a). (c) A close-up photo of one of the boreholes for the explosives.

archived in the web site of the International Working Group on Rotational Seismology (see the Data and Resources section for more information). The translational acceleration data from this experiment has been analyzed by Langston *et al.* (2009), and we plan to submit an article with analysis of the rotational velocity data in the future.

The N3 Explosion Site

The N3 explosion site is located at 24.57872° N, 121.4795° E. Two explosions were set off at 17:01 UTC (code name N3P, 3000 kg) and at 18:01 UTC (code name N3, 750 kg) on 4 March 2008. The origin times are: 17:01:17.824 and 18:01:17.988, respectively. They were determined by D. Okaya (personal comm., 2008) from the 1000 samples/sec records of the Texan Uphole Array (equipment from the Incorporated Research Institutions for Seismology Program for Array Seismic Studies of the Continental Lithosphere [IRIS PASSCAL], with 4 seismometers within 20 m of the shots). From our data alone, we deduced the origin times as 17:01:17.82 and 18:01:17.99, respectively, which agree well with the Okaya values. Figure 1a shows a Google map with the N3 explosion site and the array recording site marked and local features, such as river, road, etc., noted. A photo of the four boreholes at the N3 explosion

site is shown in Figure 1b, as viewed from the road depicted on Figure 1a. A close-up photo of one of the boreholes for the explosives is shown in Figure 1c.

For the first explosion, chemical explosives were loaded in three boreholes to a depth of 80 m, and the boreholes were separated by about 27 m. For the second explosion, chemical explosives were loaded in only one borehole to a depth of 60 m, and this borehole is about 27 m from the center borehole for the first explosion. Locations of the two shot points (N3P and N3) and the array recording stations are shown in Figure 2a. The first station (N01) is about 250 m, the center array is about 500 m, and the last station (N11) is about 600 m from the shot points, respectively. Figure 2b is an enlargement of the center array, where the interstation spacing is about 5 m for stations N03 to N09. Stations N03, N05, N06, N07, and N09 were equipped with the R-1 rotational sensors in addition to the accelerometers.

Instrument Deployment

Planning of this recording experiment was made by Chun-Chi Liu and Willie Lee. Instruments were deployed at the array recording site in locations as shown in Figure 2, after extensive discussions with Hung-Chie Chiu, John

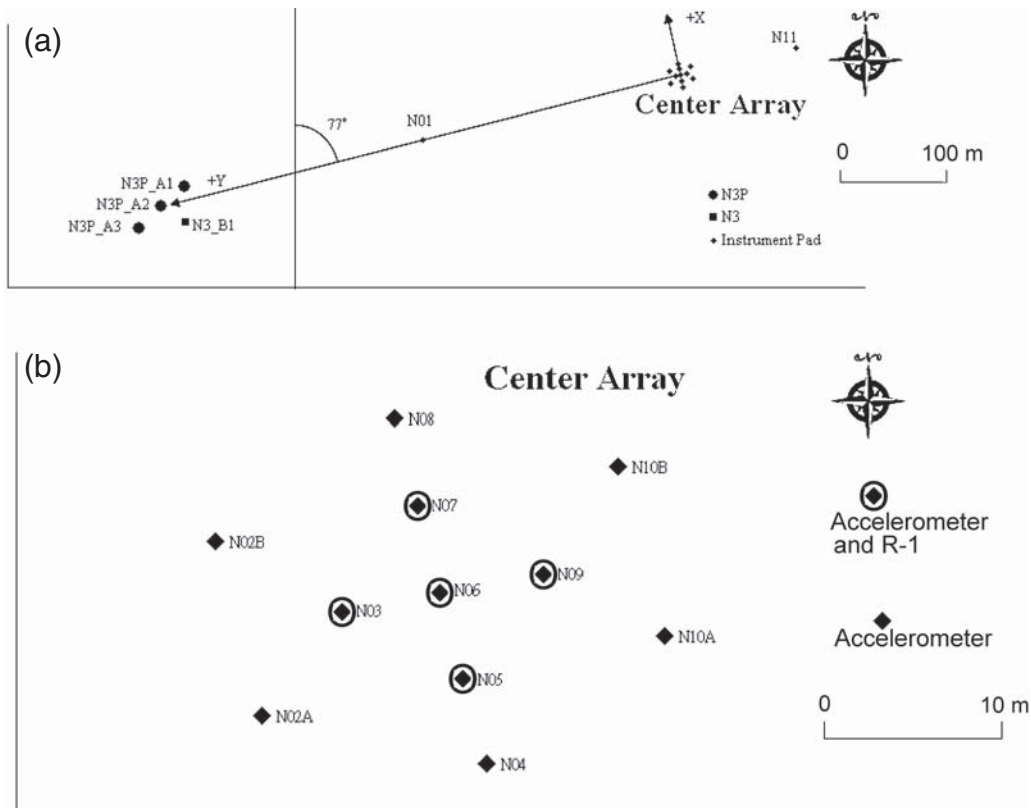


Figure 2. (a) Locations of the two shot points (N3P and N3) and the array recording stations. The N3P shot point consisted of three boreholes with explosives. (b) An enlargement of the center array, where the interstation spacing is about 5 m for stations N03 to N09. Stations N03, N05, N06, N07, and N09 were equipped with the R-1 rotational sensors in addition to the accelerometers.

Evans, Gary Fuis, Chuck Langston, Bob Leugoud, Bob Nigbor, and Paul Spudich. Although the N3 explosion site is situated in a relatively broad riverbed, we were limited in choosing a location for the instrument deployment because of the river, hills, roads, and cultivated field (see Fig. 1a). The array recording site was boxed in between a cultivated field and a steeply rising hill.

After a preliminary location for the center array was chosen, the stations were located by a precise field survey. Fortunately, the drilling rigs were tall and could be easily seen through a theodolite at 500 m distance (see Fig. 1b). A straight line from the main shot point hole (N3P_A2)

to the array center (N06) was established, and the transverse line was established by rotating the theodolite by 90° . The relative distances between stations in the center array were determined by using a measuring tape. The configuration of the center array is enlarged as shown in Figure 2b. In addition, a station (N01) at about 250 m and a station (N11) at about 600 m from the main shot hole (N3P_A2) were installed. We consulted Paul Spudich on the station spacing (h) of the center array, and he suggested using the formula $h < c/(4f_{\max})$, where c is the horizontal phase velocity of the S or surface waves, and f_{\max} is the maximum frequency that one wishes to apply the method used in Spudich *et al.*



Figure 3. (a) Photo in the vicinity of the array recording site. (b) A photo showing the center array site. To build the instrument site, (c) a big stone in the mud was first selected, and (d) a cement pad with dimensions 60×60 cm and 20 cm in depth was constructed so that sensors could be bolted onto it. (e) Instruments at station N01 are shown with a TSA-100S accelerometer, a R-1 rotational sensor, and a Gyrochip rotational sensor secured to the cement pad in the lower part of the photo. (f) A plastic box was used to hold the recording equipment.

(1995) to infer rotations (P. Spudich, personal comm., 2008). Assuming $c \sim 1.5$ km/sec and $f_{\max} = 50$ Hz, we chose $h = 5$ m.

A photo in the vicinity of the array recording site is shown in Figure 3a, and a photo of the center array site is shown in Figure 3b. Expecting large ground accelerations, we constructed cement pads for the instruments. The ground around the center array is alluvium, with a mixture of mud and stones. We first searched for a big stone in the mud (Fig. 3c) to construct a cement pad of the dimensions 60×60 cm and 20 cm in depth (Fig. 3d), so that sensors could be bolted onto it (Fig. 3e). A plastic box was used to house the recording equipment, that is, a datalogger (Model Q330 with Baler by Quanterra), battery, and excess cables (Fig. 3f).

After finishing the cement pads, we employed a professional survey company to measure precisely the relative distance of the cement pads at the array recording site and of the shot point boreholes. All distances are measured using station N06 as the Cartesian coordinate origin. We define a line from station N06 to shot hole N3P_A2 as the $+y$ axis, then the transverse direction as the x axis (see Fig. 2a). Locations of the centers of the cement pads and of the shot points are listed in Table 1. The measurement error is about ± 5 cm within the center array and about ± 10 cm outside the center array.

Twelve six-channel, 24 bit dataloggers with Global Positioning System (GPS) receivers, 13 triaxial accelerometers, and 8 triaxial rotational sensors were deployed. Instrument information is summarized in Table 2.

Instrument Calibrations

Because of a hurried schedule, we did not calibrate all the sensors before deployment, but all sensors were calibrated after the recording.

Dataloggers

A total of 12 dataloggers (9 Q330 and 3 Q330HR by Quanterra) were used to record the two explosions that took place near local midnight. The Q330 datalogger has six channels with 24 bit resolution, and the Q330HR has 3 channels with 26 bit resolution and 3 channels with 24 bit resolution. Because we had more recording channels than we needed, we did not use the 26 bit channels for ease of data processing. The dataloggers were turned on to record continuously in the late afternoon before the shots and were removed the following morning. We set the sampling rate at the maximum rate allowed by the Q330, that is, 200 samples/sec. We used individual GPS receivers in continuous mode for timing purposes.

Accelerometers

Thirteen triaxial accelerometers were deployed: eight TSA-100S sensors from Metrozet (Metrozet, 2007) and five Episensor ES-T sensors from Kinemetrics (Kinemetrics, Inc., 2005). The amplitude response of these two types of accelerometers is flat from direct current (d.c.) to the -3 dB corner frequencies of 225 and 200 Hz, respectively. Through the tilt gravity calibration method, we calculated the d.c. sensitivity of the TSA-100S and compared them to the factory

Table 1
Station Information

Station Code*	TWD97 System			Coordinate Origin at N06	
	Latitude (°)	Longitude (°)	Elevation (m)	x (m)	y (m)
N01	24.5792222	121.4818722	391.193	-0.027	246.493
N02A	24.5796500	121.4841583	385.462	-5.105	10.130
N02B	24.5797417	121.4841361	385.289	5.129	10.125
N03	24.5797056	121.4841972	385.357	-0.011	5.016
N04	24.5796250	121.4842667	385.367	-10.133	0.028
N05	24.5796694	121.4842556	385.321	-5.127	0.030
N06	24.5797167	121.4842444	385.106	0.000	0.000
N07	24.5797611	121.4842333	384.893	5.103	0.005
N08	24.5798056	121.4842222	384.666	10.163	0.004
N09	24.5797250	121.4842944	385.012	-0.033	-5.114
N10A	24.5796917	121.4843528	385.023	-5.087	-10.100
N10B	24.5797806	121.4843306	384.617	5.124	-10.086
N11	24.5799222	121.4853111	381.641	-1.602	-110.390
Shot Boreholes					
N3P_A1	24.5788694	121.4796722	397.932	11.451	472.234
N3P_A2	24.5787194	121.4794611	397.648	0.000	497.008
N3P_A3	24.5785528	121.4792639	398.698	-13.721	520.424
N3_B1	24.5785944	121.4796833	397.763	-18.518	478.139

The N3P shot has three boreholes loaded with explosives. The N3 shot is a single-hole shot. See text for explanation of the x - y coordinate system.

*The column titled Station Code includes the shot boreholes.

Table 2
Instrument Information

Station	Q330 [†] S/N	Baler S/N	Sensor A [‡] (Channels 1–3) Model (S/N)	Sensor B [‡] (Channels 4–6) Model (S/N)
N01	1869	6704	TSA-100S (497)	R-1 (A201505)
N02A	1862	5180	EpiSensor ES-T (1610)	
N02B	1862	5180		EpiSensor ES-T (841)
N03	2705	6092	TSA-100S (498)	R-1 (A201507)
N04	HR2562	6182		TSA-100S (493)
N05	296	6047	TSA-100S (491)	R-1 (A200415)
N06	1870	6091	TSA-100S (469)	R-1 (A201504)
N07	1857	5181	TSA-100S (444)	R-1 (A200414)
N08	HR2509	6209		TSA-100S (433)
N09	1876	1297	TSA-100S (494)	R-1 (A201506)
N10A	1716	6770	EpiSensor ES-T (1609)	
N10B	1716	6770		EpiSensor ES-T (843)
N11	1858	5791	EpiSensor ES-T (844)	R-1 (121)
N12 [§]	HR2568	6761		GyroChip

[†]The datalogger's resolution (Model Q330) is 24 bits, the sampling rate was set at 200 samples/sec, and the sensitivity is 419,430 digital counts/volt.

[‡]Sensor A is the input into channels 1–3 of the datalogger.

[‡]Sensor B is the input into channels 4–6 of the datalogger.

[§]Station N12 was colocated with station N01.

values as shown in Table 3. The EpiSensor ES-T sensitivities are given in Table 4.

R-1 Rotational Sensors

Besides one GyroChip rotational sensor, a total of seven R-1 rotational sensors were deployed. They were manufactured by eentec and consisted of two R-1 sensors (serial number [S/N] A200414 and A200415) purchased in 2004, one R-1 sensor borrowed from the Central Weather Bureau (S/N 121, purchased in 2006), and four R-1 sensors purchased in 2008 (eentec, 2008).

The R-1 is a direct triaxial rotational velocity sensor with the highest sensitivity for its price in the commercial market. The principle of operation is electrochemical. The sensor element consists of a toroidal cavity and is completely filled with an electrolyte. A microporous ceramic plug containing four platinum grid electrodes is within the toroid.

When angular motions are applied around this axis of the toroid, a pressure differential occurs across the sensor cell, which causes the electrolyte to flow, and generates a current in the wire connected to the platinum grid.

Sensitivity Calibration and Polarity of Rotational Sensors

The R-1 rotational sensor has a fairly good specification for sensitivity and bandwidth as given by its manufacturer, eentec (eentec, 2008). However, our measured sensitivity values deviated from their nominal factory specifications by as much as 30%. Nigbor and Lee (2006) performed some preliminary tests in the fall of 2006. Very recently, Nigbor *et al.* (2009) carried out extensive tests on commercial rotational sensors and concluded that the R-1 sensor generally meets the specifications given by the manufacturer but that clip level and frequency response vary enough that more de-

Table 3
Sensitivity Values for the TSA-100S (Metrozet) Accelerometers:
Calibrated Values vs. the Factory Supplied Values

S/N	x (V/g)			y (V/g)			z (V/g)		
	Factory	Test	Diff* (%)	Factory	Test	Diff* (%)	Factory	Test	Diff* (%)
433	5.235	5.219	-0.30	4.954	4.934	-0.40	5.099	5.082	-0.33
444	5.177	5.160	-0.32	5.111	5.092	-0.37	5.017	4.998	-0.37
469	5.008	4.990	-0.35	5.019	5.004	-0.29	5.040	5.019	-0.41
491	5.008	4.993	-0.29	4.734	4.721	-0.27	5.136	5.130	-0.11
493	4.926	4.906	-0.40	5.187	5.174	-0.25	5.099	5.079	-0.39
494	5.176	5.159	-0.32	5.193	5.176	-0.32	5.132	5.114	-0.35
497	5.123	5.128	+0.09	4.992	4.996	+0.08	5.035	5.038	+0.05
498	5.105	5.091	-0.27	5.109	5.094	+0.29	5.191	5.188	-0.05

*"Diff" is the difference between the test and factory value in percent.

Table 4
Sensitivity Values for the EpiSensor ES-T
(Kinematics) Accelerometers

S/N	x Component (V/g)	y Component (V/g)	z Component (V/g)
841	9.990	9.999	9.955
843	9.979	9.978	9.955
844	9.984	9.983	9.935
1609	10.009	9.962	9.949
1610	9.993	9.972	9.946

tailed calibrations are warranted for individual units. We used a simple test to calculate its sensitivity, using a CT-EW1 calibration table manufactured by Lennartz Electronic (2006) and a computer program by Wielandt (2002) as reported by Lin and Liu (2008). However, this method determines the average sensitivity over several frequency bands, so that the total frequency response cannot be obtained. All the R-1 rotational sensors were calibrated by this method, and the results are listed in Table 5.

The seven R-1 rotational sensors were purchased from the manufacturer over three different time periods, and they are not identical models in details. Recently, Evans and International Working Group on Rotational Seismology (2009) recommended that we should have a consistent notation convention in rotational seismology and suggested the use of the right-hand rule. The polarities of our R-1 rotational sensors are consistent with the right-hand rule when their recorded data are multiplied by +1 or -1 as shown in Table 5.

We also deployed one GyroChip rotational sensor (Model QRS-11 00100-200 by Systron Donner) as Nigbor (1994) did. Its sensitivity was also calibrated and is listed in Table 5. However, it did not record any resolvable rotational motions from the two TAIGER explosions, probably due to its low sensitivity and high instrument noise. Therefore, we will not consider the GyroChip data any further.

Data Processing

The data processing procedure we used is essentially the same as that for the 1999 Chi-Chi earthquake (Lee *et al.*, 2001a,b). This included data quality assurance and preparing and adding header information to each recorded data file.

However, many data processing programs had to be modified to take into account the small tolerances in very near-field data. For example, when station spacing is in meters rather than in kilometers, three additional decimal places in latitudes, longitudes, and elevations are required. It was also important to note the sensor sensitivity for each component of every sensor, instead of using the nominal sensitivity for all three components and for all sensors of the same model type. In addition, software designed to process and to analyze translational acceleration data had to be modified to deal with the rotational velocity data. A data set, including the originally recorded files, processed data files in both binary and ASCII formats, and supporting software and information, will be archived at the web site of the International Working Group on Rotational Seismology (see the Data and Resources section for more information) for open access.

The recorded data from the field are in digital counts, and we have converted the data into physical units using information given in Tables 2, 3, 4, and 5, and the value of acceleration due to gravity at 25° N ($g = 9.79$ m/sec/sec). Following the International System of Units (Lide, 2002), the unit for translation acceleration is in m/sec/sec, and the unit for rotational velocity is in radian/sec (rad/sec). However, to avoid too many decimal places, we use milliradian/sec (mrad/sec) for rotational velocity. Translational acceleration is often called linear acceleration, or simply acceleration. Rotational velocity is also known as angular velocity.

In the technical specifications of R-1 by its manufacture, the self noise is $< 10^{-6}$ rad/sec rms, 0.05–20 Hz. If one wishes to have a signal-to-noise level to be better than 10:1, then the R-1 rotational can measure signals down to about 10^{-5} rad/sec rms, 0.05–20 Hz.

Figure 4 shows the translational acceleration data recorded from the first explosion (N3P shot). The waveforms are displayed in three columns for the x , y , and z components. The x and y component translational accelerations are about three times smaller than that of the z component, as expected from an explosion source. The x and y component waveforms are plotted with $3x$ magnification as indicated by the scale shown in the figure.

Table 5
Sensitivity Values for the Rotational Sensors from Calibration

S/N	x Component (V/rad/sec)	y Component (V/rad/sec)	z Component (V/rad/sec)	Bandwidth	Polarity
A200414*	48.68 ± 0.48	48.99 ± 0.58	48.38 ± 0.15	0.03–50 Hz	+1
A200415*	36.29 ± 0.42	37.37 ± 0.52	41.40 ± 1.26	0.03–50 Hz	+1
A201504*	48.08 ± 1.09	50.04 ± 0.67	49.85 ± 0.88	0.03–20 Hz	-1
A201505*	50.99 ± 0.11	48.76 ± 0.14	48.30 ± 1.31	0.03–20 Hz	-1
A201506*	50.57 ± 1.17	51.06 ± 0.45	53.56 ± 0.53	0.03–20 Hz	-1
A201507*	49.50 ± 1.20	46.92 ± 0.55	48.36 ± 1.22	0.03–20 Hz	-1
121†	58.85 ± 0.72	58.25 ± 0.58	61.57 ± 1.96	0.03–50 Hz	+1
GyroChip	1.48 ± 0.06	1.45 ± 0.08	1.51 ± 0.09	0.03–50 Hz	+1

*Model R-1 by ecentec.

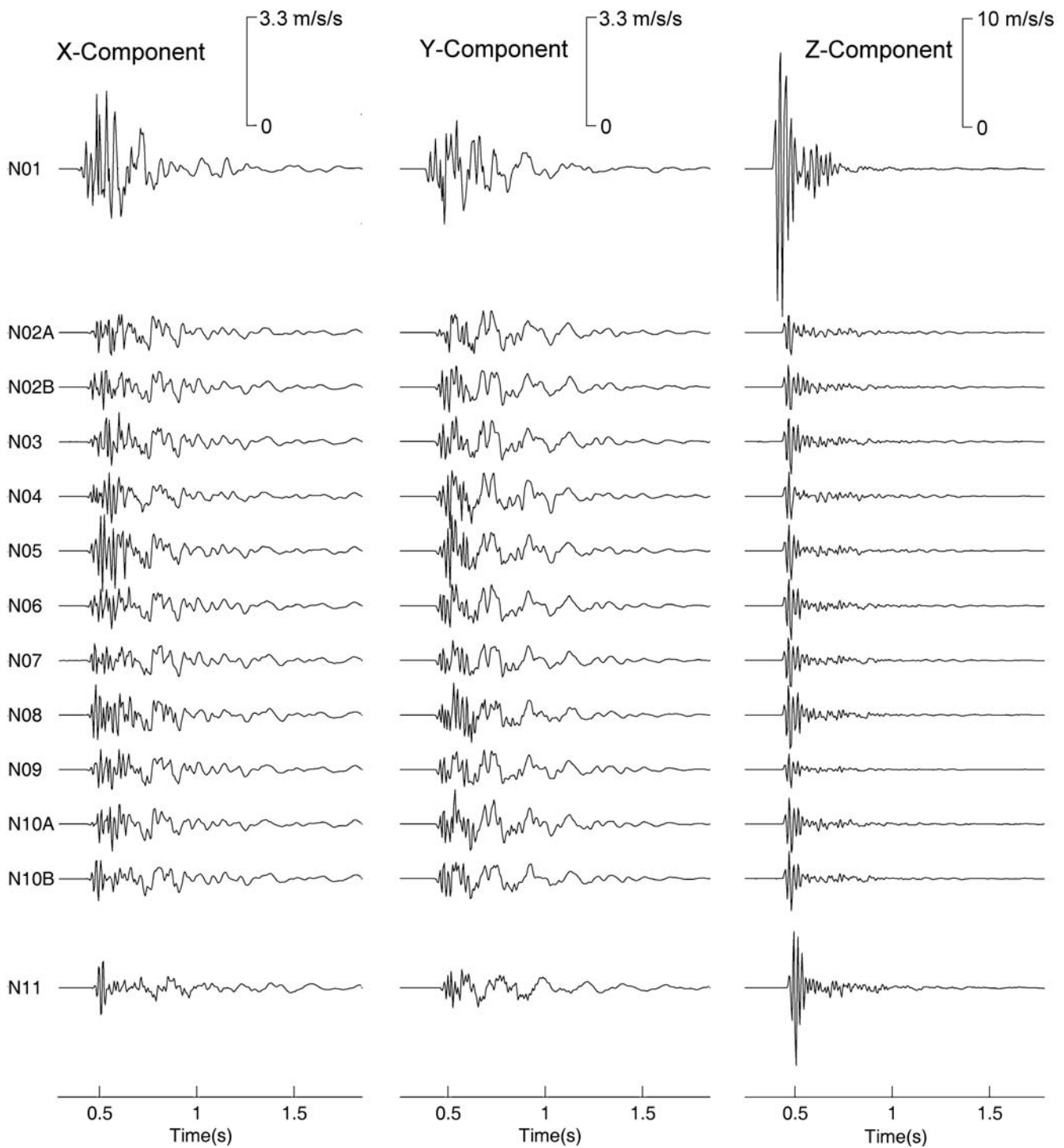


Figure 4. Translational acceleration data recorded from the first explosion (N3P). See text for explanation.

Figure 5 shows the rotational velocity data recorded from the first explosion (N3P shot). The waveforms are displayed in three columns for the x , y , and z components (i.e., angular velocity about the x , y , and z axes). The x - and y -component rotational velocities are about three times larger than that of the z component. This is expected from equation (3) because $\omega_x = \partial u_z / \partial y$ and $\omega_y = -\partial u_z / \partial x$ are derived from the larger vertical translational motions of the

explosion, and $\omega_z = \frac{1}{2}(\partial u_x / \partial y - \partial u_y / \partial x)$ is derived from the smaller horizontal translational motions of the explosion. Therefore, we plot the z -component rotational velocity with $3x$ magnification as indicated by the scale shown in the figure. This is the reverse case compared to the translational acceleration data in Figure 4. The z component of rotational velocity of station N11 is not plotted in Figure 5 because unlike that of the other six stations, it is about eight times larger

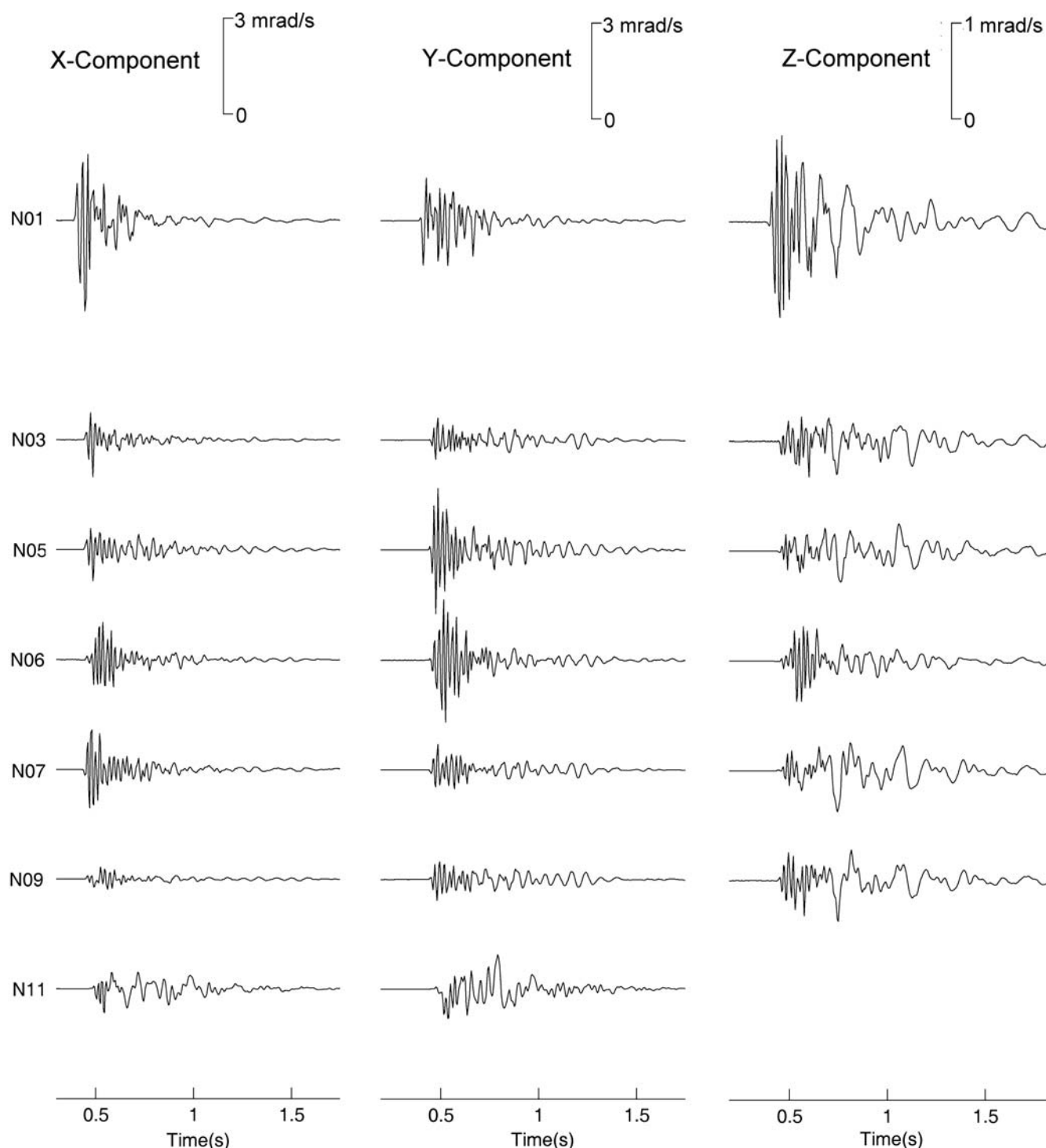


Figure 5. Rotational velocity data recorded from the first explosion (N3P). See text for explanation.

than that of the horizontal components, indicating some malfunction of this particular sensor component.

In a similar manner, the translational acceleration data and the rotational velocity data recorded from the second explosion (N3 shot) are shown in Figures 6 and 7, respectively. Because the two shot points were separated by about 27 m, distances to the recording stations are essentially the same for these two shots.

A Very Preliminary Data Analysis

The peak ground translational acceleration (PGTA) values for these two shots are given in Table 6. For ease of comparison, the PGTA values of the same component for these two shots are tabulated side-by-side. At a distance of 254 m, the largest PGTA (or peak ground acceleration as normally used in seismology) observed is for the z component:

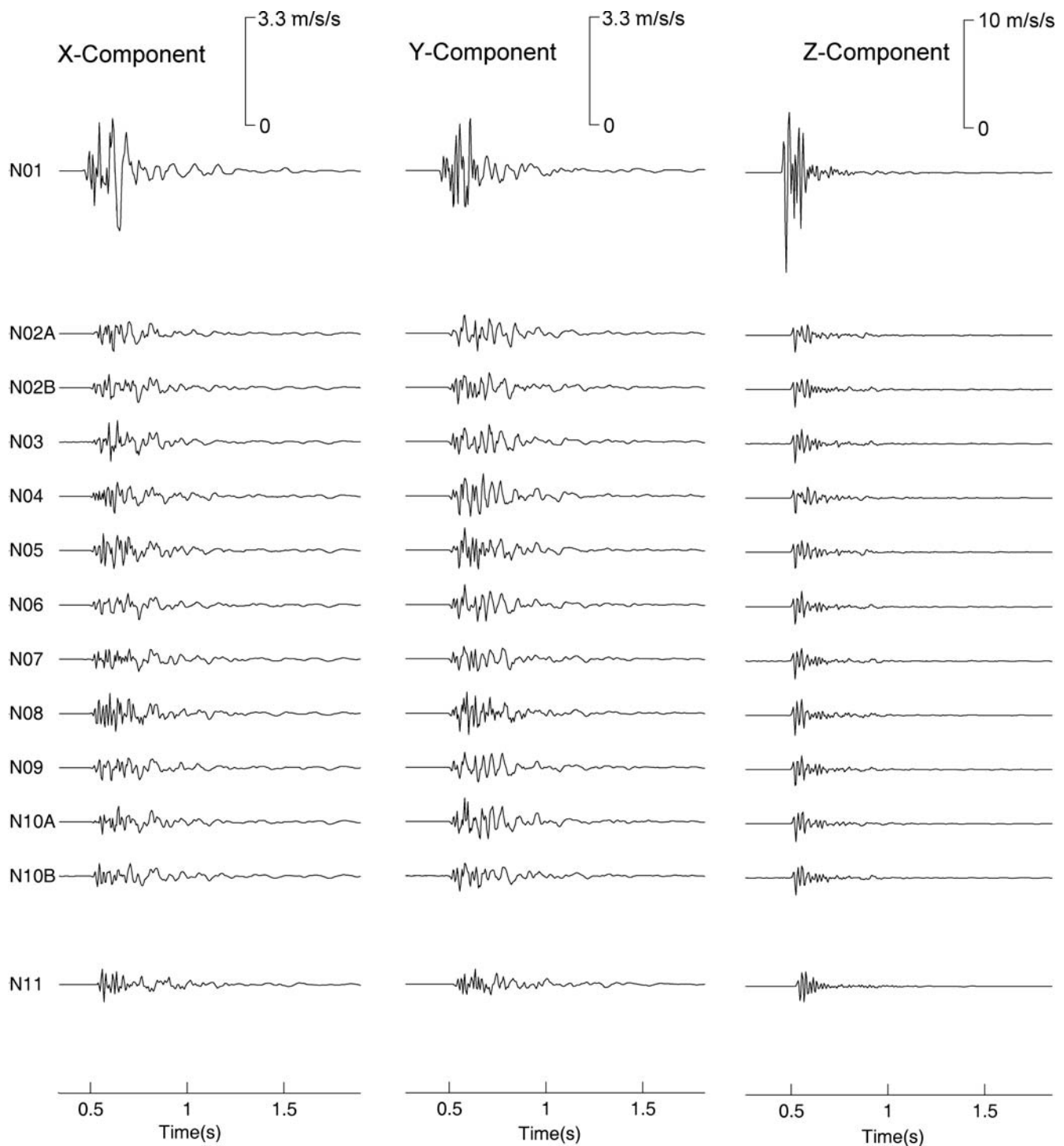


Figure 6. Translational acceleration data recorded from the second explosion (N3). See text for explanation.

13.53 and 9.18 m/sec/sec for N3P and N3 shots, respectively. Although the N3P shot used 3000 kg of explosives, four times larger than that used for the N3 shot, the PGTA values from the N3P shot are only about one and a half times larger than that for the N3 shot. One probable explanation is that because three boreholes were used in the N3P shot, the explosives of these holes (with 1000 kg of explosives each)

might not have been set off simultaneously. Because of three boreholes, there is radiation pattern associated with the N3P shot. The center array is about 28° from the line of explosives and is thus not located optimally because seismic waves should be maximum leaving perpendicular to the line.

Not only the PGTA values vary (by tens of percents) from station to station in the center array but also the whole wave-

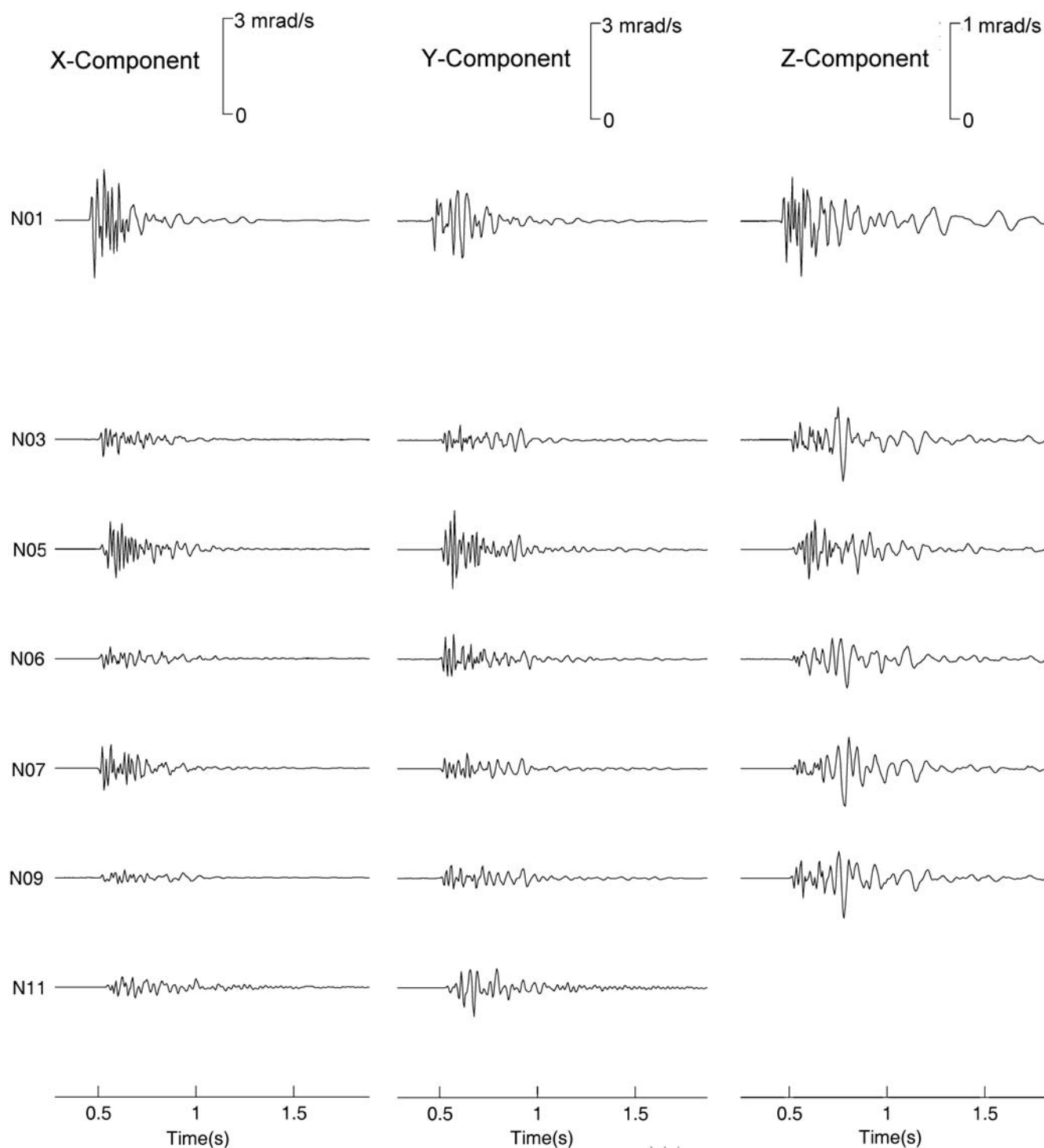


Figure 7. Rotational velocity data recorded from the second explosion (N3). See text for explanation.

forms, although the station spacing is about 5 m. This may imply that the seismic wave propagation is very complex, especially because the array recording site is boxed in a river bed with steeply rising hills on both sides. It may also imply that the PGTA values may not be a good parameter to characterize ground motions.

The peak ground rotational velocity (PGRV) values for these two shots are given in Table 7. For ease of comparison,

PGRV values of the same component for these two shots are tabulated side-by-side. At a distance of 254 m, PGRV is largest for the x component: 2.74 and 1.75 mrad/sec for N3P and N3 shots, respectively. Nigbor (1994) observed a peak rotational velocity of 38 mrad/sec at 1 km distance from a very large (1 kton) chemical explosion at the Nevada Test Site. Our largest observed rotation velocity for a single-hole shot is about 22 times smaller than Nigbor's value for an ex-

Table 6
Peak Ground Translational Acceleration (PGTA in m/sec²/sec)
for the N3P and N3 Shots

Station Code	Distance (m)	x Component		y Component		z Component	
		N3P Shot	N3 Shot	N3P Shot	N3 Shot	N3P Shot	N3 Shot
N01	253.9	2.375	1.843	1.685	1.603	13.532	9.183
N02A	488.2	0.691	0.548	0.669	0.556	2.066	1.556
N02B	488.2	0.690	0.452	0.759	0.515	2.027	1.639
N03	493.3	0.899	0.662	0.768	0.526	2.961	1.772
N04	498.3	0.869	0.534	0.952	0.623	2.254	1.423
N05	498.3	1.239	0.553	1.123	0.750	2.662	1.472
N06	498.3	0.703	0.461	0.649	0.611	3.090	1.597
N07	498.3	0.487	0.363	0.632	0.386	2.424	1.657
N08	498.3	0.909	0.617	1.003	0.658	3.008	1.868
N09	503.3	0.616	0.394	0.595	0.467	3.294	1.461
N10A	508.3	0.825	0.484	1.050	0.731	2.615	1.670
N10B	508.3	0.674	0.389	0.610	0.471	2.932	1.566
N11	608.2	0.812	0.531	0.614	0.461	3.666	1.432

plosion that was more than 1000 times larger in the amount of explosives. However, our observations were at a much closer distance (i.e., 250 m versus 1000 m). Hence, our results appear to agree with Nigbor's in an order-of-magnitude type comparison.

Although the N3P shot used 3000 kg of explosives, the PGRV values are not too much larger than the PGRV values for the N3 shot, which used only 750 kg of explosives. The PGRV values of stations in the central array also vary greatly, although the station spacing is only about 5 m.

Translation acceleration and corresponding spectra from the N3 shot, as recorded at station N06 are plotted in Figure 8 (left-hand panels). The spectra plot indicates that the z component of translational acceleration is dominant from about 32 to 55 Hz, and the sharp fall off starting at about 80 Hz is due to sampling at 200 samples/sec. The rotational velocity and corresponding spectra from the N3 shot, as recorded at station N06 are also plotted in Figure 8 (right-hand panels). The spectra plot indicates that the x component of rotational velocity is dominant from about 40 to 60 Hz, and the sharp fall off starting at about 80 Hz is due to sampling at 200 samples/sec. According to Nigbor *et al.* (2009), the amplitude response of the R-1 sensor is flat from about 0.1 to 20 Hz, and therefore, we may not have the proper instrument

to record the rotational motions of explosions that generate high-frequency waves.

Spudich *et al.* (1995) and Spudich and Fletcher (2008) developed a method to infer rotational ground motions from translational acceleration data of an array. We just started using Spudich's software to compute rotational velocity of an area defined by stations N03, N05, N07, and N09, with station N06 in the middle (see Fig. 2b). The inferred and the observed vertical rotation velocity do not compare well, and the inferred values are about a factor of 3 greater than the observed values. A likely explanation is that we have not corrected for the instrument response of the R-1 sensor, and the R-1 instrument response is such that waves of frequencies above 20 Hz are not well recorded. A proper and more thorough analysis is required, but it is beyond the scope of the present article.

Wassermann *et al.* (2009) carried out a recording experiment at a distance of about 250 m from the demolition of a 50 m high building in Munich, Germany, using a seven-element seismic array with one R-1 rotational sensor at the array center. Unlike the explosions in Taiwan, 150 kg of explosives was fired sequentially to reduce ground shaking during the demolition of the building, and the seismic waves observed were at much lower frequency (1–8 Hz). They ob-

Table 7
Peak Ground Rotational Velocity (PGRV in mrad/sec) for the N3P and N3 Shots

Station Code	Distance (m)	x Component		y Component		z Component	
		N3P Shot	N3 Shot	N3P Shot	N3 Shot	N3P Shot	N3 Shot
N01	253.9	2.741	1.750	1.362	1.123	0.966	0.563
N03	493.3	1.124	0.525	0.680	0.453	0.362	0.420
N05	498.3	1.503	0.876	2.524	1.185	0.491	0.301
N06	498.3	1.217	0.716	0.758	0.472	0.401	0.370
N07	498.3	0.708	0.353	1.462	0.775	0.268	0.303
N09	503.3	0.370	0.235	0.627	0.394	0.410	0.408
N11	608.2	0.728	0.329	1.043	0.867	*	*

*Data are unavailable due to equipment malfunction.

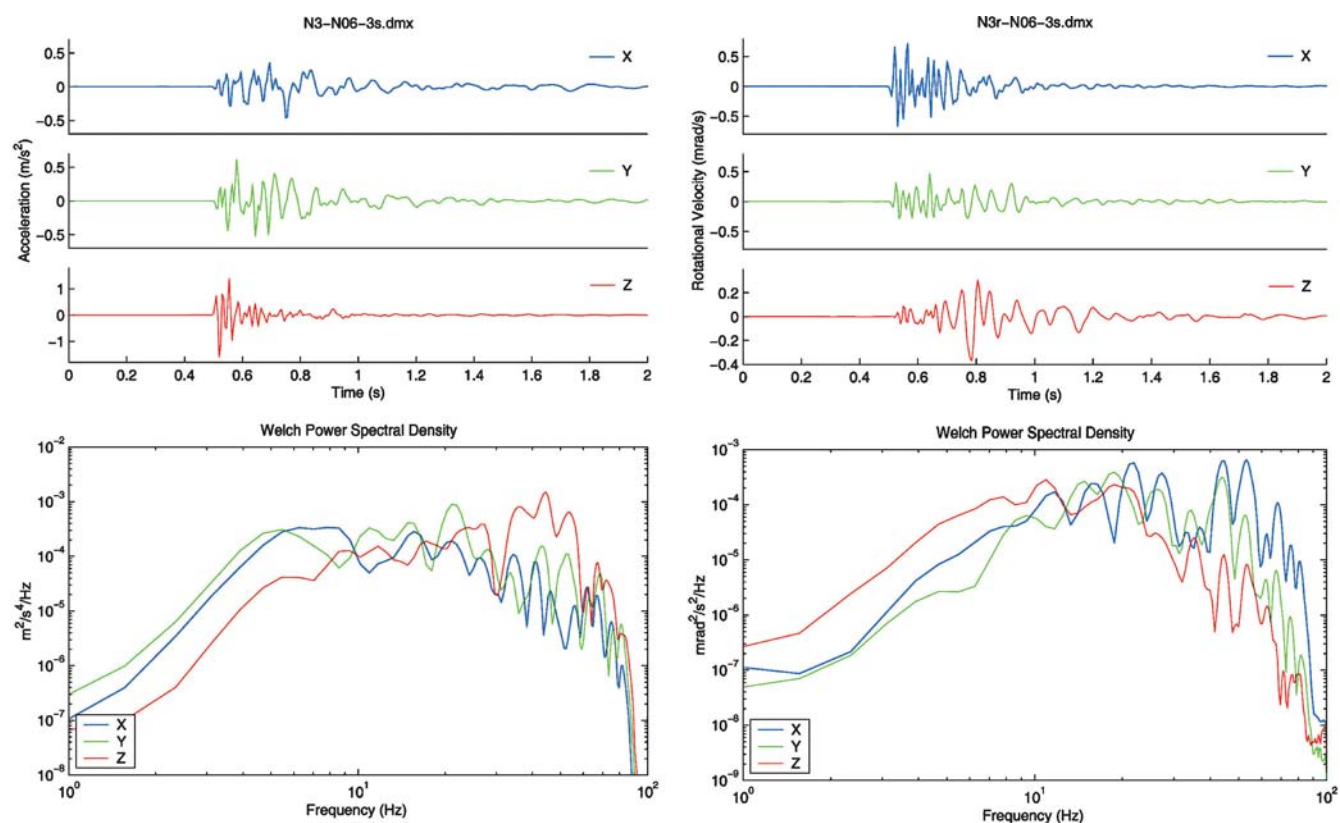


Figure 8. Translation acceleration and corresponding spectra from the N3 shot, as recorded at station N06 (left-hand panels), and rotational velocity and corresponding spectra (right-hand panels). Please note that the instrument response of the R-1 rotational sensor is flat from about 0.1 to 20 Hz, so that the spectra in the right-hand panel are not reliable outside this frequency band. See text for explanation.

tained good agreement between the computed and measured rotation motions. The peak translation acceleration they observed is about 0.04 m/sec/sec, and the peak rotational velocity is about 0.05 mrad/sec. These peak values are about 2 orders of magnitude smaller than those we observed.

Conclusions

We succeeded in recording both translational and rotational ground motions from two TAIGER explosions in northeastern Taiwan. Although the N3P shot used 3000 kg of explosives, four times larger than that used for the N3 shot, the PGTA and PGRV values from the N3P shot are only about one and a half times larger than that for the N3 shot. Large variations (tens of percents) of translational acceleration and rotational velocity were observed at stations with 5 m spacing. At a distance of 254 m, PGRV is largest for the x component: 2.74 and 1.75 mrad/sec for N3P and N3 shots, respectively. Nigbor (1994) observed peak rotational velocity of 38 mrad/sec at 1 km distance from a very large (1 kton) chemical explosion at the Nevada Test Site. Although we do not know how to scale rotational velocity with explosion size and distance from the source, our results appear to agree with Nigbor's in an order-of-magnitude type comparison.

The translational acceleration and rotational velocity data of our field experiment offer many subarray station configurations to compare measured point rotational motions with areal rotational motions inferred from the translational motions recorded by an array of accelerometers. However, extensive amounts of work are required to perform the analysis properly because the instruments we deployed are not optimal for recording the two explosions in Taiwan. The Q330 dataloggers can only sample at 200 samples/sec, whereas 1000 samples/sec may be needed. The response of the R-1 rotational sensor is also limited to about 40 Hz, whereas 200 Hz may be needed.

Data and Resources

All translational and rotational seismograms described in this article were collected by ourselves and will be archived at the web site of the International Working Group on Rotational Seismology (<http://www.rotational-seismology.org/>, last accessed January 2009) for open access, and all other data used were published.

Acknowledgments

We wish to thank Hung-Chie Chiu, John Evans, Gary Fuis, Chuck Langston, Bob Leugoud, Bob Nigbor, and Paul Spudich for their suggestions and comments during the planning of the recording experiment. We

are grateful to Chien-Ying Wang for leading the TAIGER Land Active Source Experiment in Taiwan and to David Okaya for supplying us with the Texan Uphole Array data recorded at the two shot points. We thank Gray Jensen, Chuck Langston, Art McGarr, and Bob Nigbor for their valuable comments and suggestions on the manuscript draft and Doug Dodge for computer programming support. We are grateful to Erhard Wielandt for his valuable comments on calibrating rotational sensors and to Paul Spudich for providing his Strain12 computer code for computing areal rotational motions from translational motions.

References

- Bath, M. (1979). *Introduction to Seismology*, Birkhauser Verlag, Basel.
- Cochard, A., H. Igel, B. Schuberth, W. Suryanto, A. Velikoseltsev, U. Schreiber, J. Wassermann, F. Scherbaum, and D. Vollmer (2006). Rotational motions in seismology: theory, observation, simulation, in *Earthquake Source Asymmetry, Structural Media and Rotation Effects*, R. Teisseyre, M. Takeo, and E. Majewski (Editors), Springer-Verlag, Heidelberg, 391–411.
- eentec (2008). *Instruction Manual, Special Case, Model R-1 (Serial Number A200504 thru A200547)*, St. Louis, Missouri, 8 pp. (<http://www.eentec.com/>, last accessed January 2009).
- Evans, J. R., and International Working Group on Rotational Seismology (2009). Suggested notation conventions for rotational seismology, *Bull. Seismol. Soc. Am.* **99**, no. 2B, 1073–1075.
- Huang, B. S. (2003). Ground rotational motions of the 1991 Chi-Chi, Taiwan earthquake as inferred from dense array observations, *Geophys. Res. Lett.* **30**, no. 6, 1307–1310.
- Huang, B. S., C. C. Liu, C. R. Lin, C. F. Wu, and W. H. K. Lee (2006). Measuring mid- and near-field rotational ground motions in Taiwan, A poster presented at the 2006 Fall AGU Meeting, San Francisco.
- Kinematics, Inc. (2005). *User Guide: EpiSensor Force Balance Accelerometer Model FBA ES-T*, Pasadena, California (ftp://ftp.kmi.com/pub/software_manuals/301900/301900D.pdf, last accessed January 2009).
- Langston, C. A., W. H. K. Lee, C. J. Lin, and C. C. Liu (2009). Seismic-wave strain, rotation, and gradiometry for the 4 March 2008 TAIGER explosions, *Bull. Seismol. Soc. Am.* **99**, no. 2B, 1287–1301.
- Lee, W. H. K., T. C. Shin, K. W. Kuo, K. C. Chen, and C. F. Wu (2001a). CWB free-field strong-motion data from the 21 September Chi-Chi, Taiwan, earthquake, *Bull. Seismol. Soc. Am.* **91**, 1370–1376.
- Lee, W. H. K., T. C. Shin, K. W. Kuo, K. C. Chen, and C. F. Wu (2001b). Data files from CWB free-field strong-motion data from the 21 September Chi-Chi, Taiwan, earthquake, *Bull. Seismol. Soc. Am.* **91**, 1390, and CD-ROM supplement.
- Lennartz Electronic (2006). *The CT-EW1 Calibration Table*, Document Number: 990-0062, Lennartz Electronic GmbH, Tübingen, Germany (<http://www.lennartz-electronic.de/>, last accessed January 2009).
- Lide, D. R. (Editor) (2002). *CRC Handbook of Chemistry and Physics*, Eighty-third Ed., CRC Press, Boca Raton.
- Lin, C. J., and C. C. Liu (2008). Calibrating the R-1 rotation sensors on CT-EW1 Table, Institute of Earth Sciences Report IESER2008-001, Academia Sinica, Taipei, Taiwan.
- Metrozet LLC (2007). *Triaxial Seismic Accelerometer TSA-100S: User's Manual*, Torrance, California (<http://www.metrozet.com/>, last accessed January 2009).
- Nigbor, R. L. (1994). Six-degree-of-freedom ground motion measurement, *Bull. Seismol. Soc. Am.* **84**, 1665–1669.
- Nigbor, R. L., and W. H. K. Lee (2006). A preliminary evaluation of the R-1 rotational sensor, a report posted online at: <http://www.rotational-seismology.org/> (last accessed January 2009).
- Nigbor, R. L., J. R. Evans, and C. R. Hutt (2009). Laboratory and field testing of commercial rotational seismometers, *Bull. Seismol. Soc. Am.* **99**, no. 2B, 1215–1227.
- Spudich, P., and J. B. Fletcher (2008). Observation and prediction of dynamic ground strains, tilts, and torsions caused by the *M* 6.0 2004 Parkfield, California, earthquake and aftershocks derived from UPSAR array observations, *Bull. Seismol. Soc. Am.* **98**, 1989–1914.
- Spudich, P., L. K. Steck, M. Hellweg, J. B. Fletcher, and L. M. Baker (1995). Transient stresses at Parkfield, California, produced by the *M* 7.4 Landers earthquake of June 28, 1992: observations from the UPSAR dense seismograph array, *J. Geophys. Res.* **100**, no. B1, 675–690.
- TAIWAN Integrated GEodynamics Research (TAIGER) (2008). *TAIGER (TAIWAN Integrated GEodynamics Research) Project for Testing Models of Taiwan Orogeny*, <http://taiger.binghamton.edu/> (last accessed January 2009).
- Takeo, M. (1998). Ground rotational motions recorded in near-source region of earthquakes, *Geophys. Res. Lett.* **25**, 789–792.
- Wassermann, J., S. Lehndorfer, H. Igel, and U. Schreiber (2009). Performance test of a commercial rotational motions sensor, *Bull. Seismol. Soc. Am.* **99**, no. 2B, 1449–1456.
- Wielandt, E. (2002). Seismometry, in W. H. K. Lee, H. Kanamori, P. C. Jennings, and C. Kisslinger (Editors), *International Handbook of Earthquake and Engineering Seismology, Part A*, Academic Press, Amsterdam, 283–304.

Institute of Earth Sciences
Academia Sinica
P.O. Box 1-55, Nankang
Taipei, 115, Taiwan
(C.-J.L., C.-C.L.)

862 Richardson Court
Palo Alto, California, 94303
lee@usgs.gov
(W.H.K.L.)

Manuscript received 9 July 2008